Ultrasonics Sonochemistry 89 (2022) 106134

Contents lists available at ScienceDirect

Ultrasonics Sonochemistry

journal homepage: www.elsevier.com/locate/ultson

Effect of ultrasonic far-infrared synergistic drying on the characteristics and qualities of wolfberry (*Lycium barbarum* L.)

Qian Zhang, Fangxin Wan, Zepeng Zang, Chunhui Jiang, Yanrui Xu, Xiaopeng Huang *

College of Mechanical and Electronical Engineering, Gansu Agricultural University, Lanzhou 730070, China

ARTICLE INFO

Keywords:
Far-infrared
Ultrasound
Wolfberry
Drying kinetics
Quality
Microstructure

ABSTRACT

This study investigated the effects of ultrasonic frequency, ultrasonic power, irradiation height and temperature on the drying characteristics, quality and microstructure of wolfberry by ultrasonic-assisted far-infrared drying. By fitting five commonly used thin-layer drying mathematical models, it was found that the coefficient of determination (R^2) of the Weibull model was 0.99400–0.99825, the root mean square error (RMSE) was 1.2162 $\times 10^{-4}$–4.5209 $\times 10^{-4}$, and the reduced chi-square (χ^2) was 0.00207–0.00663, which was the best fit. Under the application of ultrasound, the average drying rate of wolfberry increased. Compared with natural drying, the polysaccharide content increased by 33.2 % at 250 mm irradiation height, and the total phenol content increased by 44.9 % at 40 kHz ultrasonic frequency. The antioxidant activity was the strongest, and the total flavonoids content was the highest (2.594 mg/g) at 24 W ultrasonic power. By comparing the microstructure of wolfberry under different drying methods, such as a fresh sample, natural drying, hot air drying, and ultrasonic-assisted drying, we found that the ultrasonic assistance increased the number of micropores on the surface of wolfberry, reduced the damage to epidermal cells, reduced the mass transfer resistance of the drying process and accelerated the drying process. This study shows that ultrasonic-assisted far-infrared drying technology played a significant role in the heat and mass transfer of wolfberry drying, and had great potential in the commercial processing of wolfberry.

1. Introduction

Wolfberry (*Lycium barbarum* L.) belongs to the genus Lycium of Solanaceae. It has health effects, such as promoting glucose and lipid metabolism, improving optic nerve health and improving human immunity. It is widely used in daily health care. Wolfberry has high medicinal and economic value, but fresh wolfberry moisture and sugar content adversely affect the long-term storage and transportation, thus influencing its value. Moreover, the unstable shelf-life leads to huge economic losses.

Drying is a very important preservation method in food processing. Its main function is to reduce the water activity of the product, thereby inhibiting the growth of microorganisms, and reducing chemical reactions to prolong the shelf life of a product at room temperature. At present, hot air drying [1], microwave [4], far-infrared [2,30,3], vacuum freezing-drying [5], and other drying methods have been applied to wolfberry. Infrared radiation technology belongs to internal heating, which provides consistent direction of heat and mass transfer and achieves internal and external heating simultaneously. Thus, it has the advantages of low energy consumption and high heat transfer efficiency. In the drying process, the uniform temperature distribution is maintained, and the demand for airflow in the drying process is reduced. In recent years, infrared radiation has been successfully applied to the dehydration of various agricultural products, such as turmeric [6], apple [7], stevia [8], and kiwifruit [9]. However, although far-infrared technology has significant effect on heat transfer in the drying process, it has little effect on promoting mass transfer because of its limitations. Therefore, it is necessary to adopt some effective methods to strengthen the role of mass transfer to improve the dehydration rate and quality of products.

Ultrasonic wave is an elastic mechanical wave that can produce mechanical effects, cavitation effects, and thermal effects in the drying process [10]. An effective method to accelerate the mass transfer process, it can change the medium structure, enhance the liquid turbulence and reduce the mass transfer resistance in the solid–liquid system, thus effectively promoting the transfer and migration of water. In previous studies, ultrasonic-assisted hot air drying significantly shortened the drying time of carrots, had a positive impact on the quality and color of

* Corresponding author.
E-mail address: huangxp@gsau.edu.cn (X. Huang).

https://doi.org/10.1016/j.ultsonch.2022.106134
Received 6 June 2022; Received in revised form 15 August 2022; Accepted 19 August 2022
Available online 24 August 2022

carotenoids, and had a great impact on total phenolic compounds [11]. The application of hot air drying on persimmon [12] can significantly shorten the drying time and result in significant changes in the color andrehydration rate value. There are three commonly used ultrasound technologies, which are, ultrasonic pretreatment, gas-medium ultrasound, and direct-contact ultrasound. Used for the drying process, direct-contact ultrasound has a stronger strengthening effect on the drying process than ultrasonic pretreatment. Additionally, direct-contact ultrasound can directly transfer the ultrasonic energy to the material, which is more efficient than gas-medium ultrasonic energy. Studies revealed that ultrasound combined with far-infrared radiation, could reduce the dehydration rate and improve the quality of jackfruit during drying [13]. Moreover, it could improve the porous structure of bananas, enhance the heat and mass transfer processes and accelerate water migration and diffusion [14]. In addition, it could reduce the color difference of potato slices, decrease the hardness and brittleness and the contents of total phenols and flavonoids were increased [15].

This study intends to study the effects of different drying temperatures, irradiation height, ultrasonic power and ultrasonic frequency on the drying characteristics of wolfberry by adopting ultrasonic and far-infrared technology, and then evaluate the effects of quality and microstructure changes in order to provide technical guidance for the postpartum processing of wolfberry.

2. Materials and methods

2.1. Materials

The wolfberries used in this experiment were purchased from the Zhongning wolfberry plantation in Ningxia(Ning Xia, Chian). The variety was Ningqi No. 1, and the average initial moisture content was 79 ± 2 %. It was stored at 2–4 °C before the experiment.

2.2. Infrared-ultrasound dryer

The ultrasonic infrared radiation dryer used in this experiment was jointly developed by the School of Mechanical and Electrical Engineering of Gansu Agricultural University (Lan Zhou, China) and Tianshui Shenghua Microwave Technology Co., ltd. (Tian Shui, China). The sketch of the equipment structure is shown in Fig. 1.The equipment

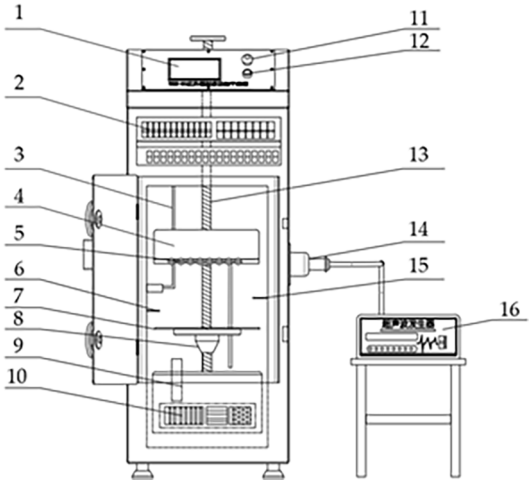

Fig. 1. Contact ultrasonic synergistic vacuum far infrared radiation dryer. (1) control panel; (2) electric control box; (3) exhaust port; (4) stents; (5) infrared radiation tube; (6) temperature sensor 1; (7) ultrasound vibration board; (8) ultrasonic transducer; (9) automatic weighing module; (10) pneumatic system and vacuum pump; (11) switch; (12) auxiliary heating switch; (13) lifting screw; (14) aviation converter; (15) temperature sensor 2; (16) ultrasonic generator.

mainly included a far-infrared heating system, ultrasonic system, and control system. The infrared heating power ranged from 0 to 3000 W. The adjustable frequency of ultrasonic generator was 25 kHz, 28 kHz, and 40 kHz, and the maximum power was adjustable to 0–100 W. The infrared heating tube was adjusted using the manual adjustment wheel, and the distance between vibration plate ranged from 100 to 500 mm. The ultrasonic parameters were adjusted by the ultrasonic generator. The stainless-steel vibration plate was fixed above the ultrasonic vibrator. The ultrasonic energy emitted by the ultrasonic transducer was directly transmitted to the material through the vibration plate.

2.3. Experimental methods

The drying temperature (45 °C, 50 °C, and 55 °C), irradiation height (250 mm, 300 mm, and 350 mm), ultrasonic frequency (25 kHz, 28 kHz, and 40 kHz), ultrasonic power (12 W, 24 W, and 36 W, 48 W, and 60 W) were selected as the experimental factors. Wolfberry was brought to room temperature (22 ± 1 °C) 1 h before the experiment. Wolfberries with no surface damage and similar shape and size were selected as the raw materials. Samples were weighed in each 100 ± 0.5 g group. The fresh wolfberry was soaked in 4 % Na_2CO_3 solution for 3 min to remove the wax layer on the surface and drain the surface water. When the weight was the same before and after soaking, the wolfberries were evenly spread on the vibration plate for drying. The weight of the sample was measured every 30 min until a water content of 10 % was achieved.

Control experiment (natural drying): An empty space exposed to sunlight was selected. The stacked objects were laid and flattened in the empty space, so that the stacked objects were flat. Next, the mesh cover with holes was expanded and laid on the stacked objects. Wolfberries was stacked in the mesh cover, and then flattened for drying.

All the test procedures involved in this experiment are shown in Fig. 2.

2.4. Measurement of test indicators

2.4.1. Determination of moisture content of dry base

$$X = \frac{M_t - M_d}{M_d} \tag{1}$$

where X represents dry basis moisture content, %; M_t represents the weight of wolfberry at time t, g; M_d represents the dry weight of wolfberry, g.

2.4.2. Drying rate measurement

$$DR = \frac{M_{t_2} - M_{t_1}}{t_2 - t_1} \tag{2}$$

where DR represents drying rate, g/s; $M_{t2,}$ M_{t1} represents the weight of wolfberry at the moment of t_2 and t_1, g; t_2-t_1 represents the time interval between two weighing, min.

2.4.3. Determination of moisture ratio

$$MR = \frac{M_t - M_e}{M_c - M_e} \tag{3}$$

where M_t represents the dry basis moisture content of wolfberry at moment t, %; Mc represents the initial moisture content of wolfberry, %; Me represents the moisture content of wolfberry dried to equilibrium, %.

The equilibrium moisture content is relatively small in experiments so that MR term can be simplified as:

$$MR = \frac{M_t}{M_c} \tag{4}$$

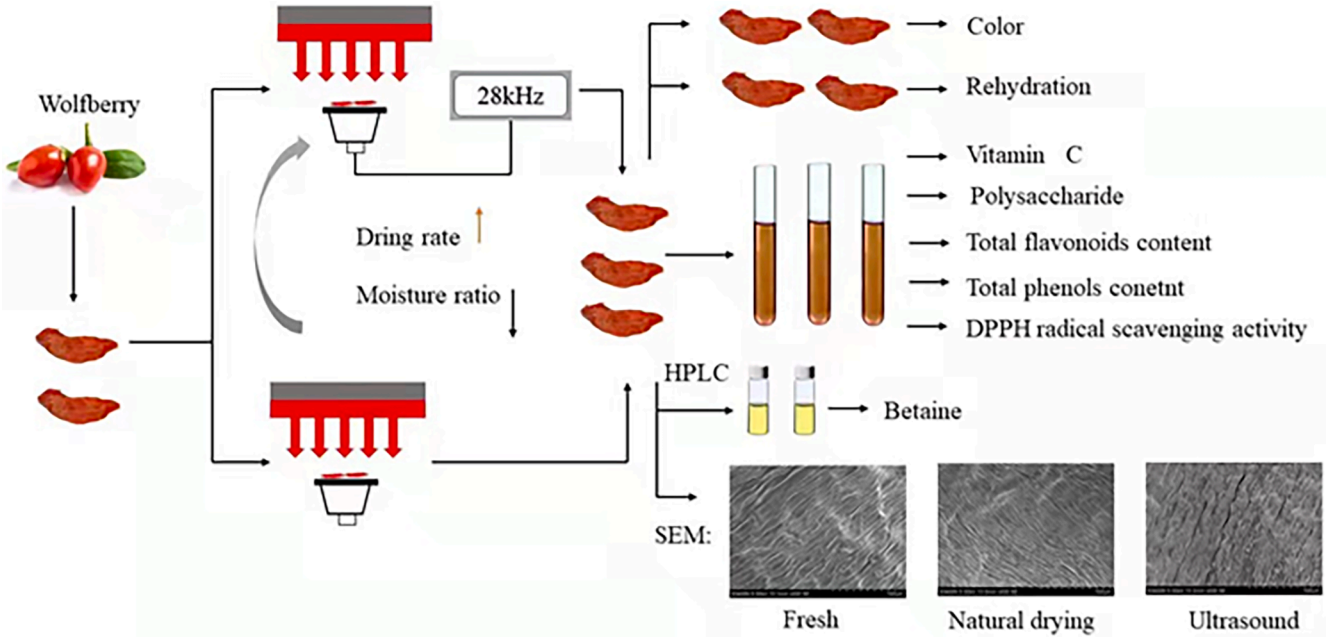

Fig. 2. Direct touch ultrasonic far infrared drying and quality testing of wolfberry schematic.

2.5. Model analysis

In order to study the moisture change pattern of wolfberry in the process of ultrasonic synergistic far-infrared drying, five common drying kinetic models were selected to fit the experimental data. The model equations are shown in Table 1.

The coefficient of determination (R^2), root mean square error (RMSE) and chi-squared value (χ^2) were chosen as the evaluation indexes of the fitting results, which were calculated as follows:

$$R^2 = 1 - \frac{\sum_{i=1}^{N}(MR_{exp,i} - MR_{pre,i})^2}{\sum_{i=1}^{N}(\overline{MR_{exp,i}} - MR_{pre,i})^2} \quad (5)$$

$$RMSE = [\frac{1}{N}\sum_{i=1}^{N}(MR_{pre,i} - MR_{exp,i})^2]^{\frac{1}{2}} \quad (6)$$

$$\chi^2 = \frac{\sum_{i=1}^{N}(MR_{pre,i} - MR_{exp,i})^2}{N - n} \quad (7)$$

where $MR_{pre,i}$ is the model-predicted moisture ratio, $MR_{exp,i}$ is the value of the moisture ratio obtained from drying experiments, MR is the average value of the experimental moisture ratio, N is the number of observations, and n is the number of constants.

2.6. Determination of color difference

The color of the sample was measured using a colorimeter. L* represents brightness, a* represents red (+) or green (−), and b* represents yellow (+) or blue (−). Based on these parameters, the total color variation (ΔE) is calculated as follows:

Table 1
Five common drying kinetic models.

Model names	Model equations	Model paraments
Henderson and Pabis	MR = a·exp(-kt)	a;k
Wang and Singh	MR = 1 + a·t + bt2	a;b
Page	MR = exp(-ktm)	K;m
Weibull	MR = exp[-(t/a)b]	a;b
Iogarithmic	MR = a·exp(-kt) + c	a;k;c

$$\Delta E = \sqrt{(\Delta L^*)^2 + (\Delta a^*)^2 + (\Delta b^*)^2} \quad (8)$$

where $\Delta L^* = L - L^*$; $\Delta a^* = a - a^*$; $\Delta b^* = b - b^*$;

where ΔE represents the total color difference of the sample; L^*, a^*, and b^* represent the brightness, red-green, and yellow-blue values of fresh wolfberry, respectively; L, a, and b represent the brightness, red-green, and yellow-blue values of dry products, respectively.

2.7. Determination of polysaccharide content

2.7.1. Preparation of test samples

The preparation of the extract was slightly changed on the method of [30]. 1 g sample was accurately weighed and placed in the mortar. 50 mL ethanol was added according to the solid–liquid ratio of 1: 5 (m/V). The extract was grinded into slurry under ice bath conditions and transferred into 50 mL centrifuge tube. The supernatant was centrifuged for 10 min at 4 °C and 4000 r / min after shaking for 48 h in a constant temperature shaker whose parameter is 120 r / min under dark conditions.

2.7.2. Measurement method

The polysaccharide content was determined by phenol sulfate method [16]. In the experiment, 5 μL of sample extract was taken into the test tube and added 1.0 mL of 9.0 % phenol into it. After mixing evenly, 3.0 mL of concentrated sulfuric acid was added. The mixture was placed at room temperature for 30 min and then determined. The absorbance of the reaction system at 485 nm was recorded for three times, with no sample solution as a blank control. According to the above operation, the standard curve of polysaccharide content was obtained with sucrose as reference substance.

According to the absorbance value, the mass concentration of polysaccharide in the corresponding mixture was determined on the standard curve, and the polysaccharide content in wolfberry was calculated by the Formula(9):

$$\text{Retention of polysaccharide} = \frac{V_2 C_1}{V_1 M} \quad (9)$$

where C_1 represents sucrose concentration, g / g; V_1 represents the

volume of sample extract used in titration, mL; V_2 represents the total volume of sample extract, mL; M represents sample quality, g.

2.8. Determination of total phenol content

2.8.1. Preparation of test samples

Preparation of the extract was the same as ' 2.7.1 '.

2.8.2. Determination method

Total phenol content was determined by Folin-Ciocalteu method reagent [17]. In the experiment, 300 μL of sample extract was put into the test tube and then 2.0 mL of 10 % Folin-Ciocalteu and 1.0 mL of 7.5 % Na_2CO_3 were successively added. The mixed sample was placed at 37 °C for 60 min in dark and then determined. The absorbance of the reaction system at 760 nm was recorded for three times, with no sample solution as a blank control. According to the above operation, the standard curve of total phenol content was obtained with gallic acid as reference substance.

According to the absorbance value, the mass concentration of total phenol in the corresponding mixture was determined on the standard curve, and the total phenol content in wolfberry was calculated by the Formula(10):

$$\text{Retention of total phenol} = \frac{V_2 C_2}{V_1 M} \tag{10}$$

where C_2 represents gallic acid mass concentration, mg/g; V_1 represents the volume of sample extract used in titration, mL; V_2 represents the total volume of sample extract, mL; M represents sample quality, g.

2.9. Determination of total flavonoids content

2.9.1. Preparation of test samples

Preparation of the extract was the same as ' 2.7.1 '.

2.9.2. Determination method

The content of total flavonoids was determined by sodium nitrite-aluminum nitrate-sodium hydroxide method [18]. In the experiment, 1200 μL sample extract was put into the test tube, and 2.0 mL distilled water and 0.3 mL 5 % $NaCO_3$ solution were added in turn. After mixing for 5 min, 0.3 mL 10 % $AlCl_3$ was added to mix for 1 min, and 2.0 mL 1 mol / L NaOH was added to mix for uniform determination. The absorbance of the reaction system at 510 nm was recorded for three times, with no sample solution as a blank control. According to the above operation, the standard curve of total flavonoid content was obtained with catechin as the reference substance.

According to the absorbance value, the mass concentration of total flavonoids in the corresponding mixture was found on the standard curve, and the content of total flavonoids in wolfberry was calculated by the formula (11):

$$\text{Retention of total flavonoids} = \frac{V_2 C_3}{V_1 M} \tag{11}$$

where C_3 represents catechin concentration, mg/g; V_1 represents the volume of sample extract used in titration, mL; V_2 represents the total volume of sample extract, mL; M represents sample quality, g.

2.10. Oxidation resistance

2.10.1. Preparation of test samples

Preparation of the extract was the same as ' 2.7.1 '.

3. Determination method

Total antioxidant capacity of organic active substances was determined by DPPH method [19]. In the experiment, 80 μL sample extract was put into the test tube, and then 3.0 mL 10^{-4} mol / L DPPH methanol solution was added into it. The mixture was placed at room temperature for 30 min in dark oscillation and then determined. The absorbance of the reaction system at 515 nm was recorded for three times. According to the above operation, 70 % ethanol was used as blank control and 500 μmol / L 90 % ascorbic acid methanol solution was used as positive control.

$$\text{DPPH radical scavenging activity} = \frac{A_0 - A}{A_0} \times 100\% \tag{12}$$

where A is the absorbance value of the sample solution; A_0 is the absorbance value without sample solution.

3.1. Determination of vitamin C

3.1.1. Preparation of test samples

1.0 g sample was accurately weighed and placed in the mortar, and then 20 mL 50 g / L trichloroacetic acid solution (TCA solution) was added. After grinding into slurry under ice bath conditions, The mixture was transferred to a 100 mL volumetric flask and calibrated to scale with 50 g / L TCA solution. After mixing, centrifugation was performed at 4 °C and 1800 r/min for 10 min, and the supernatant was kept for later use.

3.1.2. Determination method

In the experiment, 1.0 mL sample extract was taken into the test tube, and then 1.0 mL 50 g / L TCA solution and 1 mL anhydrous ethanol were added in turn. After mixing and shaking, 0.5 mL 0.4 % phosphoric acid–ethanol solution, 1.0 mL 5 g / L phenanthroline-ethanol solution and 0.5 mL 0.3 g / L $FeCl_3$-ethanol solution were added. The mixture was reacted at 30 °C for 60 min and then determined. The absorbance of the reaction system at 534 nm was recorded for three times, with no sample solution as blank control. According to the above operation, the standard curve of Vc compound content was obtained with ascorbic acid as reference substance..

According to the absorbance value, the mass of ascorbic acid in the corresponding mixture was found on the standard curve, and the content of ascorbic acid in wolfberry was calculated by the formula (9). The content of ascorbic acid in wolfberry was expressed as the mass of ascorbic acid contained in 100 g sample (fresh weight), namely mg / 100 g. Calculation formula:

$$\text{Retention of vitamin C} = \frac{V \times m'}{V_N \times m \times 1000} \tag{13}$$

where m′ denotes the mass of ascorbic acid obtained from the standard curve, μg; V represents the volume of sample extract used in titration, mL; V_N represents the total volume of sample extract, mL; m Represents sample quality, g.

3.2. Determination of betaine content

3.2.1. Chromatographic conditions

Chromatographic column: Merk RP-C18 (250 mm × 4.6 mm, 5 μm); mobile phase: acetonitrile–water (83: 17, V / V); flow rate: 1 mL / min; column temperature: 30 °C; detection wavelength: 195 nm; injection volume: 1 μL.

3.2.2. Preparation of reference solution

A total of 4 mg betaine was precisely weighed, dissolved and diluted with appropriate amount of methanol to prepare the reference stock solution with a mass concentration of 1 mg / mL. A total of 0.5 mL of the above reference stock solution was accurately measured and then diluted with 0.5 mL of methanol to obtain the reference solution with a mass concentration of 250 μg / mL.

3.2.3. Preparation of test samples

1.0 g sample was accurately weighed and placed in the mortar, and then30 mL methanol solution was added. After grinding into slurry under ice bath conditions, the mixture was transferred into the plug triangle bottle, and then it was processed in ultrasonic cleaning machine (power: 100 W; frequency: 40 kHz; time: 25 min). After filtration, the supernatant was centrifuged in 10 mL centrifuge tube and filtered by 0.45 μm filter membrane.

3.3. Microstructure analysis

The dried products obtained under different drying conditions were cut into 2 × 2 mm samples, which still contained high moisture after drying. The samples were fixed with 2.5 % glutaraldehyde for 30 min before electron microscopy to stabilize and solidify its microstructure. The samples were dehydrated with 50 %, 70 %, 80 %, and 90 % ethanol for 10 min each and dehydrated with anhydrous ethanol three times for 10 min each. Finally, the material was immersed in 100 % pure *tert*-butanol for 15 min and then placed in a vacuum freeze-drying machine [20]. After treatment, the sample was fixed on the SEM sample table with conductive tape, and the surface of the sample was coated for 50 s with an ion sputtering coating instrument. Then, the accelerated voltage of the electron microscope was set to 5.0 kV, and the sample was observed under the scanning electron microscope. The magnification was ×500. Representative field of vision was selected for microscopic imaging.

3.4. Statistical analysis

Each group of experiments was repeated in triplicate, and the mean values are presented. The obtained data were analyzed by Excel, Origin 18.0, and SPSS 22.0 statistical software.

4. Results and analysis

4.1. Analysis of drying characteristics

4.1.1. Effect of drying temperature on drying characteristics

The effects of different drying temperatures on drying characteristics at 300 mm irradiation height, 36 W ultrasonic power, and 28 kHz ultrasonic frequency are shown in Fig. 3. The observation curve shows the water ratio decreased with increasing temperature. The higher the temperature, the faster the average drying rate was and the less drying time required. When the temperature was 45 °C, 50 °C and 55 °C, the drying time of wolfberry (10 % water content) was 720 min, 510 min, and 420 min, respectively. Compared with 45 °C, the drying time at other temperatures was shortened by 17.6 % and 41.6 %, respectively, indicating higher temperature had a significant positive effect on reducing the dehydration time. This is because the internal phase water content of the material is relatively high in the early stage of drying, and the water evaporation rate on the surface of wolfberry is fast. Moreover, during the drying process, higher temperature can produce more heat flow, thereby increasing the temperature difference between the drying product and the drying medium. This results in an increase in the heat transfer rate. At the same time, the increase in temperature can improve the vapor pressure difference between the material and the drying medium, so as to accelerate the mass transfer rate and shorten the drying time. As the drying process progressed, the moisture content of wolfberry decreased, the water content of the internal body phase decreased greatly, and the bound water was retained. This resulted in an increase in internal water diffusion resistance and a decrease in the drying rate. In addition, infrared radiation heating and drying are directly related to the processes of emitting and absorbing infrared radiation. According to Kirchhoff's law, for a certain radiation wavelength, the radiation ability of an object is proportional to its absorption ability at the same temperature. Therefore, the higher the temperature, the higher the radiation and absorbed radiation energy of the wolfberry itself, thus improving the thermal efficiency and drying rate, and shortening the drying time. Other studies have also shown that increasing the temperature of radiation or increasing the intensity of radiation energy can shorten the dehydration time [21].

4.1.2. Effect of irradiation height on drying characteristics

The effects of different irradiation heights on drying characteristics at 50 °C, 36 W ultrasonic power, and 28 kHz ultrasonic frequency are shown in Fig. 4. The observation curve showed that the required time under different irradiation heights was 420 min, 510 min, and 690 min, respectively. Compared with the radiation height of 350 mm, the required time for drying wolfberry at 300 mm and 250 mm was shortened by 26 % and 39.1 %, respectively. The lower the irradiation height, the faster the drying rate and the shorter the dehydration time are. In addition, longer dehydration time is required as the irradiation height increases. This is because more time is required for the infrared radiation emitted by the infrared lamp to be absorbed by the moisture inside the material is, thus weakening the heat and mass transfer rate inside the material. Therefore, the evaporation rate of free water is slow. Lower irradiation height can provide higher radiation power and heat energy. Far-infrared is more easily absorbed by water inside the material. With the internal temperature increasing, the flow rate of water in the capillary and cell gap accelerates.

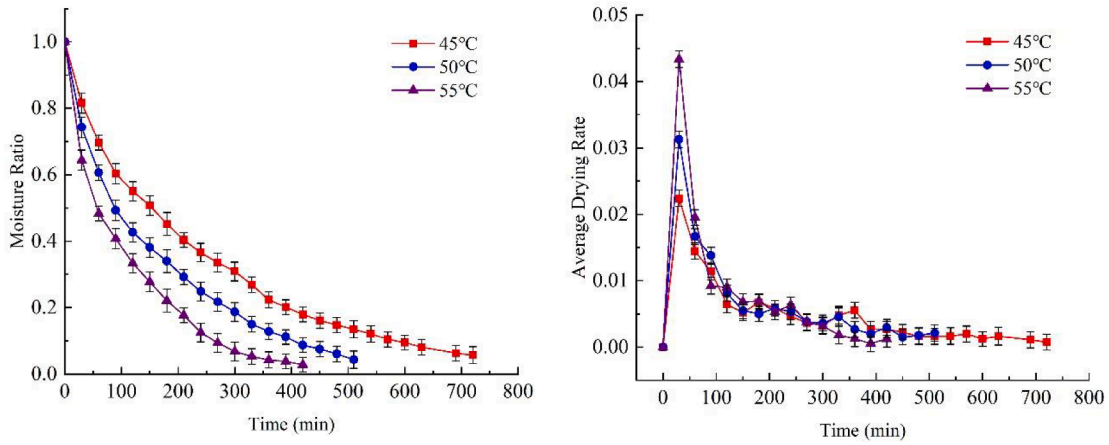

(a) (b)

Fig. 3. Effect of different drying temperatures on the drying characteristics of wolfberry.

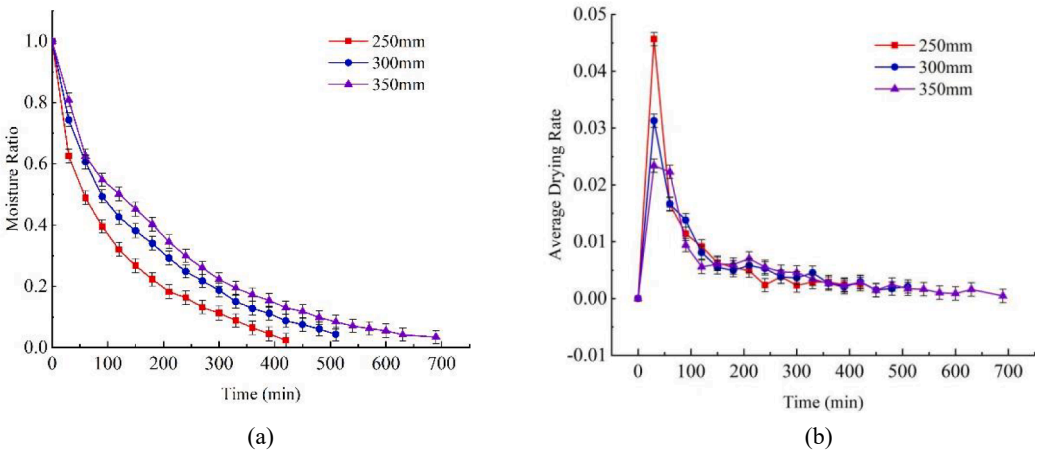

Fig. 4. Effect of non-irradiation height on the drying characteristics of wolfberry.

4.1.3. Effect of ultrasonic power on drying characteristics

The effects of different ultrasonic power on drying characteristics at 50 °C, 300 mm irradiation height, and 28 kHz ultrasonic frequency are shown in Fig. 5. From observation of curve, it can be found that the higher the ultrasonic power, the shorter the time used for drying the material to below the safe moisture content, the more obvious the corresponding strengthening effect..This is because more ultrasonic energy is produced as ultrasonic power increases. When propagating in the liquid, the cavitation effect causes bubbles on the surface of wolfberry. After a series of changes, such as oscillation, compression, expansion, and collapse, a large microjet is produced at the moment of closure or rupture, which reduces the thickness of the boundary layer of mass and heat transfer, improves the heat transfer rate, and enhances the internal water diffusion rate of wolfberry. When the power was 12 W and the drying time was 630 min, the strengthening effect was obviously weaker than at other powers. This may be because the power density at this parameter (0.12 W/g) is not sufficient to have a significant effect on the internal water fluidity of wolfberry, and its strengthening effect is limited. When the power was 48 W, the drying time was the shortest, which may be due to the stronger mechanical effect and cavitation effect of at this power. The presence of more microporous channels increases the effective water diffusion coefficient of water molecules, reduces the mass transfer resistance, and promotes the flow of water from the interior to the surface of wolfberry.

4.1.4. Effect of ultrasonic frequency on drying characteristics

The effects of different ultrasonic frequencies on drying characteristics at 50 °C, 300 mm irradiation height, and 36 W ultrasonic power are shown in Fig. 6. Accroding to the curve, when the ultrasonic frequency was 40 kHz, the dehydration process was accelerated, and the drying time was the shortest (22 % shorter than at 25 kHz). This may be because the ultrasonic propagation exceeded the attractive forces of liquid molecules, and the cavitation effect formed bubbles in the fluid at a high enough frequency. These bubbles were distributed throughout the entire liquid and expanded to a critical size. Internal explosion led to the accumulation of energy in the hot spot, resulting in extreme temperature and pressure. In the cavitation area, very high shear energy waves and turbulence were generated, which reduced the adhesion of water and increased the ability of mass and heat transfer. Therefore, the migration and diffusion of water was accelerated [22]. At the same time, when the ultrasonic wave propagates, the drying medium will convert the acoustic energy into heat energy, improve the internal energy and activity of water molecules, accelerate the heat and mass transfer rate, and then accelerate the water diffusion. Thus, the drying process is controlled by internal diffusion.

4.2. Model analysis

4.2.1. Drying process fitting results of different models

When R^2 is closer to 1, RMSE and χ^2 are closer to 0, the model prediction effect is better. Origin18.0 was used for nonlinear fitting of the five common mathematical models, and the R2, RMSE and χ^2 of each model were obtained as shown in Table 2. It can be seen that among the five selected drying kinetic models, the coefficient of determination R^2

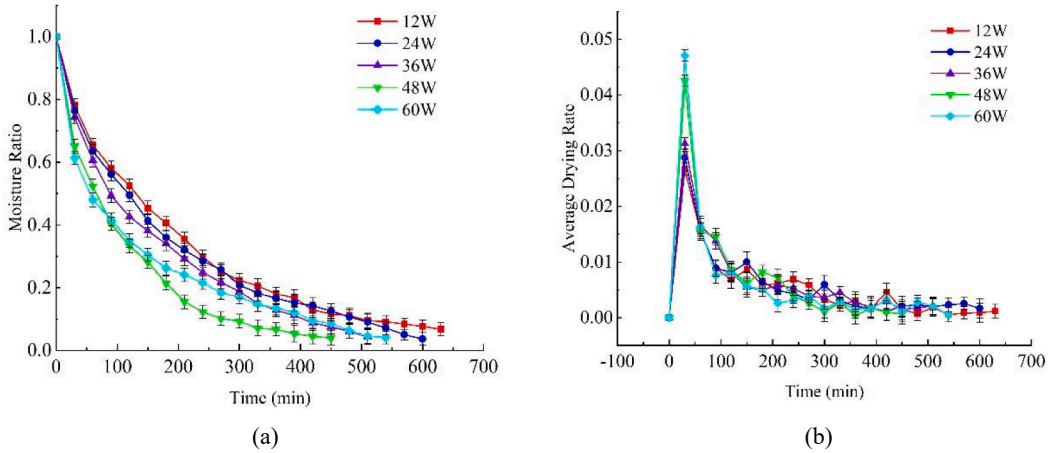

Fig. 5. Effect of different ultrasonic power on the drying characteristics of wolfberry.

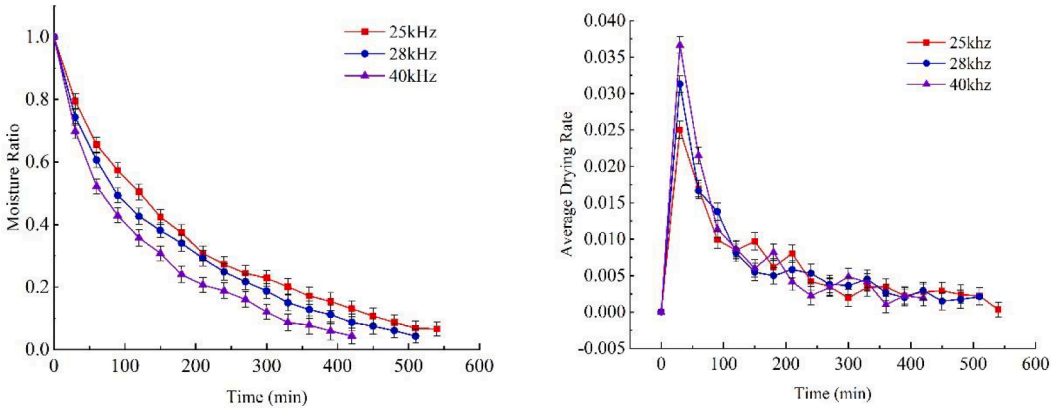

Fig. 6. Effect of different ultrasonic frequencies on the drying characteristics of wolfberry.

of the Weibull and Page models ranged from 0.99400 to 0.99825, the root mean square error RMSE ranged from 1.2162×10^{-4} to 4.52088×10^{-4}, and the reduced chi-square χ^2 ranged from 0.00207 to 0.00663. All of them can well simulate the ultrasonic synergistic far-infrared drying process of Wolfberry. Compared with other models, the Weibull model had a coefficient of determination R^2 closer to 1, smaller RMES and χ^2, and the best fitting results.

4.2.2. Model validation

In order to verify the accuracy of the model, the verification test was carried out under the parameters of temperature 50 °C, irradiation height 300 mm, ultrasonic frequency 25 kHz and ultrasonic power 36 W. It can be seen from Fig. 7 that the fitting degree of the experimental value and the fitting value is high, that is, the model can better describe the change of moisture in the drying process.

4.3. Quality analysis

4.3.1. Changes in wolfberry color.

Color difference is an important index to describe the quality of wolfberry. Color difference is used to express the color change after drying. The smaller the color difference value, the smaller the color change. Table 3 shows the L^*, a^*, and b^* values of fresh wolfberry were 38.95, 39.30, and 25.63, respectively. In the case of ultrasound-assisted infrared drying, b* values of dried wolfberry were less than that of the fresh samples, indicating that ultrasound treatment will affect the yellowness of wolfberry. Wolfberry contains a large number of sugars and carotenoids, which are the main components responsible for the color change during the drying process. As temperature increased, the value of ΔE increased from 7.07 to 9.39. Thus, the increase in temperature had a negative effect on the color of wolfberry. This is because the frequency of infrared radiation applied to the wolfberry is consistent with the frequency of the thermal motion of the object molecule. The infrared radiation will be quickly absorbed by the molecule and transformed into the thermal motion of the molecule. The higher the temperature, the faster the caramelization and Maillard reaction rates will be, and the carotenoids will undergo oxidative degradation reactions. This leads to greater color change [24]. When the ultrasonic power increased from 12 W to 24 W, the value of L^* decreased from 41.00 to 37.79, indicating the brightness of wolfberry epidermis decreased. This may be related to browning and carotenoid degradation during the drying process [23]. In addition, the mechanical and cavitation effects of ultrasonic wave increased the intercellular space and micropore, and the material surface was seriously damaged. so the effective area in contact with the ultrasonic medium increased, leading to the increase of color difference value.

4.3.2. Polysaccharide content

The effect of different drying conditions on wolfberry polysaccharide content is shown in Fig. 8(a). The highest polysaccharide content was 0.936 g/g when the ultrasonic frequency was 28 kHz, ultrasonic power was 36 W, irradiation height was 250 mm, and temperature was 50 °C. Polysaccharides are natural macromolecular compounds with a wide range of biological activities. The polysaccharide content of dried products obtained by natural drying was 0.625 g / g. Different drying conditions had significant impacts on polysaccharide content. When the ultrasonic frequency and ultrasonic power increased, they had a positive impact. This may be because the ultrasonic power and frequency reached a certain level, which stimulated the violent vibration and fragmentation of cells in wolfberry. These changes are conducive to the release of polysaccharides. When the other conditions were unchanged, the polysaccharide content was higher than that obtained by natural drying at different temperatures, showing a trend of increasing first and then decreasing. The possible reason is that the cellulose in the raw material is further degraded into soluble polysaccharides and fibrous oligosaccharides, and the polysaccharides generated from the degradation of cellulose are more easily extracted and obtained. Therefore, the content of polysaccharides gradually increased (Zhang et al., 2012). However, when the temperature was higher than 50 °C, the miscellaneous polysaccharides in wolfberry were decomposed into monosaccharides. The Maillard and caramelization reactions were accelerated, and the content was degraded. When the temperature was too low, the drying time was long, and polysaccharides were susceptible to decomposition [25].

4.3.3. Total phenols

The effect of different drying conditions on the total phenol content of wolfberry is shown in Fig. 8(b). When the ultrasonic frequency was 40 kHz, ultrasonic power was 36 W, irradiation height was 300 mm, and temperature was 50 °C, the total phenol content was the highest at 8.042 mg/g. The total phenol content under different drying conditions was higher than that under natural drying. With the increase in ultrasonic frequency, the total phenol content increased by 26.9 %, 32.2 %, and 44.9 %, respectively. This is because the appropriate ultrasonic strengthening heating may break the covalent bonds and lead to the destruction of the polymer in the cell wall of wolfberry, which released more cell wall phenolic substances or adhesive phenolic substances, thus resulting in the extraction of more phenolic substances [26]. At the same temperature, the higher the irradiation height, the lower the total phenolic content, which may be because the longerdrying time increased the oxidation reaction time of phenolic compounds under the action of internal polyphenol oxidase and peroxidase of wolfberry, resulting in lower total phenolic content [27]. At the same irradiation height, the total phenol content decreased with increasing temperature.

Table 2
Fitting results of different drying models.

Drying conditions	Model names	Model equations	evaluating indicators		
			R^2	RMES	χ^2
45 ℃	Weibull	$MR = \exp[-(t/a)^b]$	0.99664	2.2019 × 10^{-4}	0.00484
50 ℃			0.99601	2.7399 × 10^{-4}	0.00438
55 ℃			0.99400	4.5209 × 10^{-4}	0.00588
250 mm			0.99652	2.4256 × 10^{-4}	0.00315
350 mm			0.99537	2.7399 × 10^{-4}	0.00663
25 kHz			0.99825	3.5171 × 10^{-4}	0.00207
40 kHz			0.99732	1.2162 × 10^{-4}	0.00252
12 W			0.99737	2.7399 × 10^{-4}	0.00350
24 W			0.99717	1.9420 × 10^{-4}	0.00356
48 W			0.99739	1.7491 × 10^{-4}	0.00266
60 W			0.99546	1.8728 × 10^{-4}	0.00433
45 ℃	Wang and Singh	$MR = 1 + at + bt^2$	0.94241	0.00378	0.08306
50 ℃			0.91828	0.00561	0.0898
55 ℃			0.89553	0.00788	0.10241
250 mm			0.85126	0.01037	0.13476
350 mm			0.92393	0.00519	0.10859
25 kHz			0.95074	0.00344	0.05851
40 kHz			0.90401	0.00694	0.09027
12 W			0.95519	0.00364	0.07287
24 W			0.92125	0.00522	0.09909
48 W			0.89634	0.00755	0.10566
60 W			0.73314	0.01497	0.25442
45 ℃	Henderson and Pabis	$MR = a \cdot exp(-kt)$	0.99225	0.00051	0.01118
50 ℃			0.98524	0.00101	0.01622
55 ℃			0.98243	0.00134	0.01742
250 mm			0.96990	0.00210	0.02727
350 mm			0.99005	0.00068	0.01424
25 kHz			0.99242	0.00053	0.00896
40 kHz			0.98107	0.00137	0.01781
12 W			0.99155	0.00056	0.01123
24 W			0.98840	0.00077	0.01460
48 W			0.98550	0.00106	0.01478
60 W			0.93561	0.00361	0.06139
45 ℃	Page	$MR = \exp(-kt^n)$	0.99664	2.2026 × 10^{-4}	0.00485
50 ℃			0.99601	2.7399 × 10^{-4}	0.00438
55 ℃			0.99443	4.5209 × 10^{-4}	0.00588
250 mm			0.99652	2.4256 × 10^{-4}	000,315
350 mm			0.99537	2.7399 × 10^{-4}	0.00663
25 kHz			0.99825	3.1573 × 10^{-4}	0.00207
40 kHz			0.99732	1.2165 × 10^{-4}	0.00252
12 W			0.99737	2.7399 × 10^{-4}	0.00350
24 W			0.99717	1.9420 × 10^{-4}	0.00356
48 W			0.99739	1.7495 × 10^{-4}	0.00266
60 W			0.99546	1.8733 × 10^{-4}	0.00433
45 ℃	Logarithmic	$MR = a \cdot exp(-kt) + c$	0.99572	0.00015	0.09398
50 ℃			0.98701	0.00089	0.13380
55 ℃			0.98278	0.00130	0.01557
250 mm			0.97789	0.00154	0.01850
350 mm			0.99051	0.00065	0.01295
25 kHz			0.99447	0.00038	0.00615

Table 2 (*continued*)

Drying conditions	Model names	Model equations	evaluating indicators		
			R^2	RMES	χ^2
40 kHz			0.98677	0.00096	0.01149
12 W			0.99404	0.00400	0.00753
24 W			0.99079	0.00061	0.01098
48 W			0.98995	0.00073	0.00951
60 W			0.95902	0.00230	0.03677

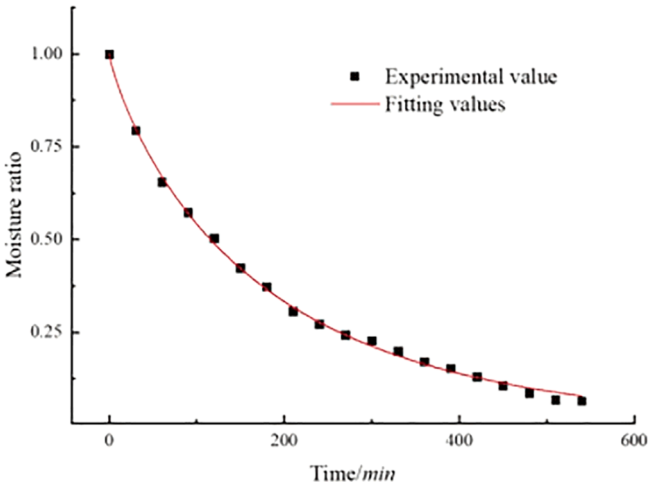

Fig. 7. Validation of the Weibull model.

Table 3
Color parameters of wolfberry under different drying conditions.

	L^*	a^*	b^*	ΔE
fresh	38.95 ± 0.53^{b}	39.30 ± 0.13^{a}	25.63 ± 0.56^{a}	
45 ℃	38.48 ± 0.37^{b}	38.18 ± 0.07^{b}	19.11 ± 0.16^{b}	7.07 ± 0.21^{b}
50 ℃	37.27 ± 0.25^{a}	37.51 ± 0.42^{c}	17.38 ± 0.20^{c}	9.14 ± 0.13^{a}
55 ℃	41.31 ± 0.03^{a}	33.72 ± 0.06^{d}	19.31 ± 0.30^{b}	9.39 ± 0.08^{a}
250 mm	37.90 ± 0.07^{a}	36.77 ± 0.65^{b}	18.79 ± 0.61^{b}	8.58 ± 0.43^{a}
350 mm	40.79 ± 1.71^{a}	38.79 ± 0.64^{a}	20.67 ± 0.93^{b}	6.80 ± 0.29^{b}
12 W	41.00 ± 0.33^{a}	34.69 ± 0.37^{c}	18.51 ± 0.57^{b}	9.44 ± 0.21^{a}
24 W	39.56 ± 0.78^{b}	39.94 ± 0.82^{a}	19.19 ± 0.28^{b}	7.14 ± 0.56^{c}
48 W	37.98 ± 0.18^{c}	39.49 ± 0.39^{a}	26.00 ± 0.01^{a}	8.49 ± 0.59^{ab}
60 W	37.79 ± 0.45^{c}	38.33 ± 0.17^{b}	18.81 ± 0.49^{b}	7.53 ± 0.25^{bc}
25 kHz	41.72 ± 0.83^{a}	32.41 ± 0.56^{c}	18.95 ± 0.40^{b}	10.70 ± 0.73^{a}
40 kHz	39.42 ± 0.43^{b}	35.61 ± 0.72^{b}	18.97 ± 0.37^{b}	8.94 ± 0.56^{b}

Note: Values followed by different letters in each column indicated significant differences ($p < 0.05$).

Additionally, the phenolic compounds had strong activity, but the chemical properties were unstable. Excessive temperature accelerated the oxidation and thermal degradation of phenolic compounds [28].

4.3.4. Total flavonoids

The effect of different drying conditions on the content of total flavonoids in wolfberry is shown in Fig. 8(c). The highest content of total flavonoids was 2.594 mg / g at an ultrasonic frequency of 28 kHz, ultrasonic power of 24 W, irradiation height of 300 mm, and temperature of 50 °C. The temperature influence diagram showed that when the drying temperature increased from 45 °C to 50 °C, the content of total flavonoids increased significantly from 1.728 mg / g to 2.295 mg / g, with an increase of 24.7 % ($p < 0.05$). This is because at higher temperature the cell components were easily decomposed, and flavonoids were released in large quantities, which increased the content of total flavonoids. However, the chemical substances of wolfberry will undergo thermal decomposition if the temperature is too high, affecting the

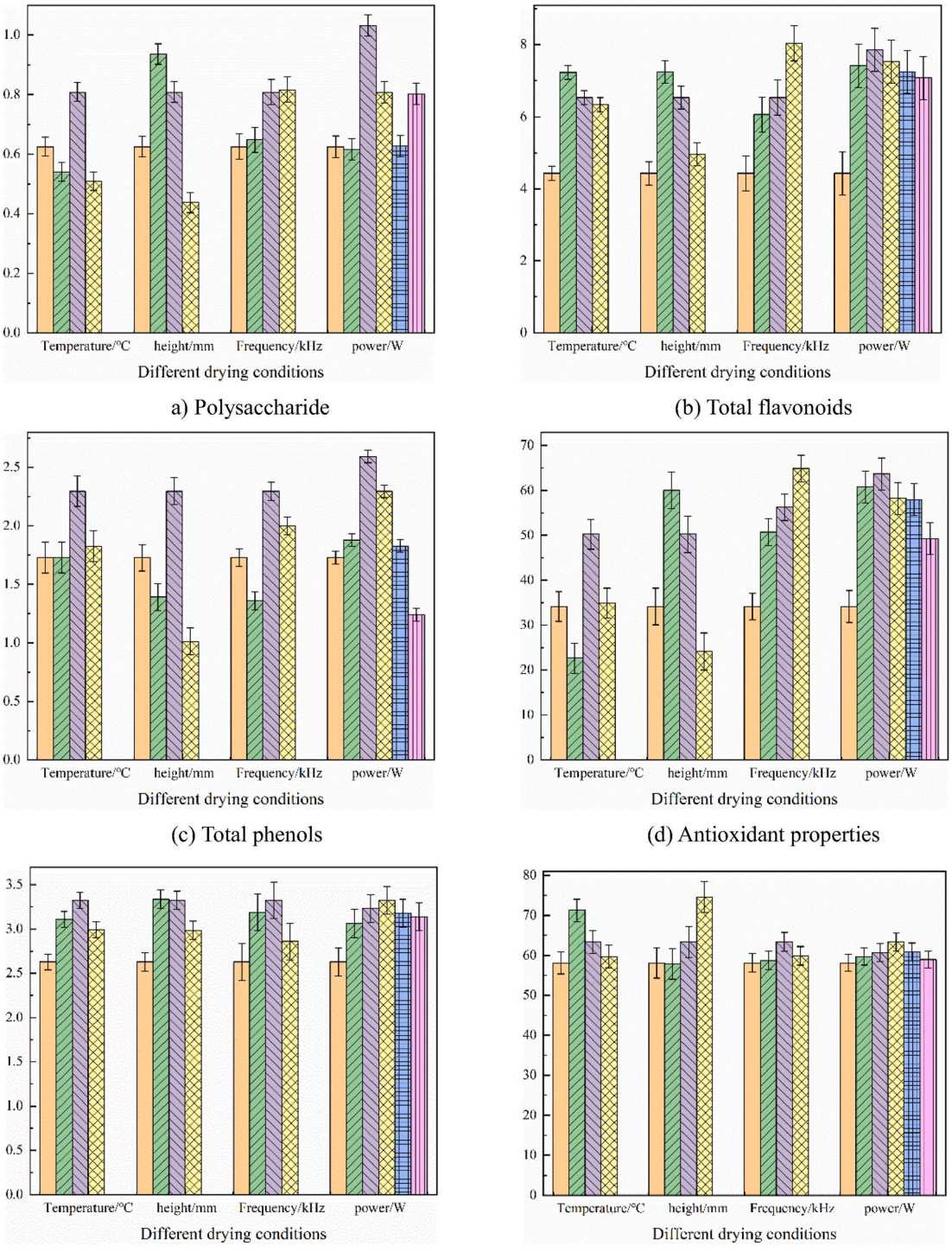

Fig. 8. Antioxidant properties, polysaccharides, total phenols, total flavonoids, vitamin C, betaine content of wolfberry under different drying conditions. Different drying conditions: natural drying (▭), 45 °C (▨), 50 °C (▨), 55 °C (▨); natural drying (▭), 250 mm (▨), 300 mm (▨), 350 mm (▨); natural drying (▭), 25 kHz (▨), 28 kHz (▨), 40 kHz (▨); natural drying (▭), 12 W (▨), 24 W (▨), 36 W (▨), 48 W (▨), 60 W (▨); Vertical bars indicate the standard deviation from the mean.

integrity of the cell structure and accelerating the degradation rate of flavonoids [9]. During the drying process, the total flavonoid content first increased and then decreased with increasing ultrasonic frequency and ultrasonic power. This is because far-infrared radiation heating stimulates the synthesis of flavonoids in wolfberry. However, owing to the mechanical effect of ultrasound, cells are broken and flavonoids are degraded.

4.3.5. Antioxidant properties

In this study, the 2,2-diphenyl-1-picrylhydrazyl (DPPH) method was used to determine the antioxidant activity of dried wolfberry. The method is based on the determination of the scavenging capacity of antioxidants on stable DPPH. The effect of different drying conditions on the content of total flavonoids in wolfberry is shown in Fig. 8(d). The highest free radical scavenging activity was 64.906 mg / g at 40 kHz ultrasonic frequency, 36 W ultrasonic power, 300 mm irradiation height, and 50 °C. As ultrasonic frequency increased, DPPH radical scavenging activity also increased significantly, compared with natural drying. At frequencies 25, 28, and 40 kHz, DPPH radical scavenging activity increased by 32.7 %, 39.3 %, and 47.3 %, respectively. A high correlation between total antioxidant activity and total phenol content has been reported previously. When the temperature was 45 °C, the drying time was long, which increased contact time between active antioxidants and air, as well as the oxidation degree. However, when the temperature was 55 °C, oxidation resistance decreased owing to the degradation of antioxidants caused by ultrasound and overheating [13].

4.3.6. Vitamin C

The effect of different drying conditions on the vitamin C content in wolfberry is shown in Fig. 8(e). The highest vitamin C content was 74.567 mg /100 g at ultrasonic frequency 28 kHz, ultrasonic power 36 W, irradiation height 350 mm, and 50 °C. In Fig. 5(e), ultrasound has a positive effect on the retention of vitamin C content. This is because the application of ultrasound shortens the drying time, shortens the contact time with oxygen, slows the degradation rate, and retains vitamin C content. As the temperature rises, the instability and thermal degradability of vitamin C and its sensitivity to humidity tended to decrease because vitamin C is unstable and easily affected by high temperature and humidity. During the drying process, the equilibrium moisture content in wolfberry decreased with increasing temperature, which increased the degradation of vitamin C [29].

4.3.7. Betaine

The effect of different drying conditions on betaine content in wolfberry is shown in Fig. 8(f). Betaine is an unstable alkaloid that readily decomposes. The betaine content was the highest (3.334 %) when the ultrasonic frequency was 28 kHz, the ultrasonic power was 36 W, the irradiation height was 250 mm, and the temperature was 50 °C. The cavitation effect and the acoustic torrent effect of ultrasonic technology strengthen the fluid turbulence at the same time, which significantly improved the heat transfer coefficient of the phase interface. Thus, moisture in wolfberry easily diffused during drying, less time was consumed, and betaine content was retained. The betaine content first increased and then decreased with increasing ultrasonic frequency and power, which may be due to higher ultrasonic parameters. As the internal moisture content of wolfberry decreased, the characteristic impedance of ultrasonic cavitation in the solid, dried material was larger than that in the internal water, which led to an increase in the attenuation coefficient of ultrasound in the propagation process. In addition, the strengthening effect of ultrasound was hindered. The betaine highest content was achieved at 250 mm irradiation height, and this may be due to the absorption of more radiation energy, which increases the drying time of wolfberry and retains more betaine components.

4.3.8. Microstructure analysis

The change in microstructure was closely related to the migration of

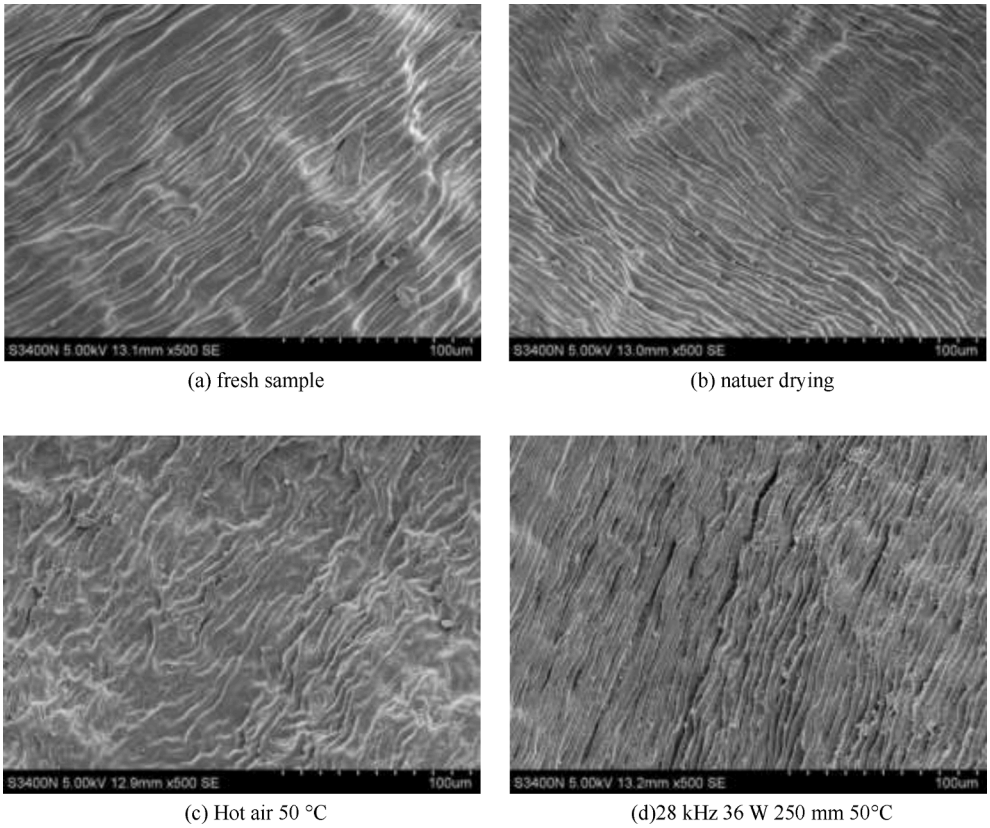

(a) fresh sample (b) natuer drying

(c) Hot air 50 °C (d)28 kHz 36 W 250 mm 50°C

Fig. 9. Microstructure under different drying methods.

water during drying. The influence of different drying methods such as ultrasonic-assisted far-infrared radiation on the surface of wolfberry is shown in Fig. 7. From the graph, the surface of fresh wolfberry samples (Fig. 9.(a)) was relatively flat, and the surface of naturally dried wolfberry (Fig. 9.(b)) was wrinkled. Hot air (Fig. 9.(c)) damages the surface microstructure of wolfberry. This is because in the process of thermal convection, there is a small heat flux inside the material, the internal moisture vaporization rate is small, and the surface moisture rapidly migrates to form a layer of hard film. The surface cells produce irregular shrinkage, and the interwoven network structure is destroyed. The cells are tightly bonded together, and the internal organizational structure will produce internal cracks [31,32,33]. Compared with the surface of wolfberry after natural drying and hot air drying, the shrinkage was aggravated under the synergistic effect of ultrasound and far-infrared radiation (Fig. 9(d)). This may be because the ultrasonic wave caused a series of physicochemical effects and deformations on the surface of the wolfberry, which helps to reduce the thickness of the surface layer, facilitates the flow of water inside the wolfberry in the far-infrared radiation, and improves the drying speed. Ni also reported similar results (Ni., 2020). Although the size of some of the pores of wolfberry after ultrasonic strengthening were large, the microstructure was uniform. Moreover, the microchannels were formed and the pores turned to be regular. Similar changes were also observed in the microphotographs of dried mango slices (Yao et al., 2020). More porous tissue is mainly due to the mechanical action of ultrasound and cavitation (Nowacka & Wedzik, 2016). These tiny micro-bubbles grow and break with the vibration of the surrounding medium and the migration of water, thus forming some new micro-channels and then providing more mass transfer paths for the water migration [5]. In addition, the perturbation effect generated by ultrasound helps to enhance the turbulent flow of water in the area of the far-infrared radiation heat source, reduces the thickness of the solid–liquid mass transfer boundary layer and the concentration gradient difference, which is beneficial to heat and mass transfer [33]. A global view of the microstructure shows that the ultrasonic wave has a great influence on the surface of the wolfberry, which in turn affects the drying rate, quality and various indicators of the wolfberry from a macroscopic level. Similar results were obtained in other studies on the effect of ultrasonic application on pineapple slices (Xu et al.,2022), saffron [34] and pear slices [28].

5. Conclusions

This study explored, the effects of ultrasound-assisted far-infrared drying on drying parameters, quality and microstructure of wolfberry. The results showed that the radiation and absorbed radiation energy of wolfberry increased with the higher temperature, which enhanced the thermal efficiency and drying rate, and shortened the drying time. The lower irradiation height provided higher radiation power and thermal energy for wolfberry, and its radiation was more easily absorbed by the internal water, elevating the internal temperature of wolfberry and accelerating the flow of water in capillaries and cell interstices. As the ultrasonic parameters increased, the strengthening effect and the internal moisture diffusion rate of wolfberry increased. Additionally, less time was required for wolfberry to reach the desired moisture content. However, when the power was too high and when drying to near safe moisture content, the characteristic impedance of the cavitation effect produced by ultrasound treatment in the solid was larger than that in the liquid, which led to the propagation of ultrasonic attenuation coefficient increase, and decrease the reinforcement. In the classical drying model, the Weibull model is the best drying kinetic model of wolfberry. Comparing the dry products processed by ultrasonic-assisted far-infrared drying with the dry products obtained by natural drying, the application of ultrasound obviously retained the content of active ingredients such as vitamin C, betaine, and other active ingredients in the dry products. The polysaccharide content of dried products was the highest (0.936 g / g) when the irradiation height was 250 mm, and the total phenol content was the highest (8.042 mg / g) when the ultrasonic frequency was 40 kHz. At 24 W, the antioxidant activity was the strongest and the total flavonoids content of dried products was the highest (2.594 mg / g). This indicated that ultrasonic enhancement not only shortened the drying time, but also had a positive effect on the retention of nutrients because it improved the quality of wolfberry dried products. By observing the microstructure through different drying methods, it was found that the use of ultrasound increased the surface micropores and enlarged the capillaries, which reduced the mass transfer resistance and made the diffusion of water inside the material easier, thus increasing the drying rate.

CRediT authorship contribution statement

Qian Zhang: Writing – original draft, Conceptualization, Formal analysis, Writing – review & editing. **Fangxin Wan:** Project administration. **Zepeng Zang:** Investigation, Formal analysis. **Chunhui Jiang:** Investigation, Formal analysis. **Yanrui Xu:** Investigation, Formal analysis. **Xiaopeng Huang:** Methodology, Investigation, Funding acquisition.

Declaration of Competing Interest

The authors declare that they have no known competing financial interests or personal relationships that could have appeared to influence the work reported in this paper.

Data availability

The authors do not have permission to share data.

Acknowledgments

The authors acknowledge the financial support provided by the National Natural Science Foundation of China (Grant No. 32160426). The authors would also like to thank Qiang Ma, who helped conducted the experiments. We thank Accdon (www.accdon.com) for its linguistic assistance during the preparation of this manuscript.

References

[1] Y. Luo, X.P. Huang, W.Q. Li, F.X. Wan, G.J. Ma, Optimization of hot air drying process for ultrasonic pretreatment of Lycium barbarum, Forestry Mach. Woodwork. Equip. 07 (2020) 47–51.
[2] L. Xie, A.S. Mujumdar, Q. Zhang, J. Wang, S. Liu, L. Deng, D. Wang, H.-W. Xiao, Y.-H. Liu, Z.-J. Gao, Pulsed vacuum drying of wolfberry: effects of infrared radiation heating and electronic panel contact heating methods on drying kinetics, color profile, and volatile compounds, Drying Technol. 35 (11) (2017) 1312–1326.
[3] F.X. Wan, W.Q. Li, Y. Luo, B. Wei, X.P. Huang, Effect of ultrasonic pretreatment on the characteristics and quality of far-infrared vacuum drying of Lycium barbarum, Chinese Herbal Med. 51 (18) (2020) 4654–4663.
[4] Ma, L. Q. (2015). Research and experiment on microwave drying characteristics of Lycium barbarum (Master's thesis, Ningxia University).
[5] P. Sun, C.L. Li, Y.M. Yang, Q.C. Wu, Experiments on the production of active Lycium barbarum by vacuum freeze-drying, Food Sci. 10 (1994).
[6] A.J. Fernando, C. Gunathunga, T.J. Brumm, S. Amaratunga, Drying turmeric (curcuma longa l.) using far-infrared radiation: drying characteristics and process optimization, J. Food Process Eng. 44 (4) (2021), https://doi.org/10.1111/jfpe.13780.
[7] H.S. El-Mesery, G. Mwithiga, Performance of a convective, infrared and combined infrared- convective heated conveyor-belt dryer, J. Food Sci. Technol. 52 (5) (2015) 2721–2730, https://doi.org/10.1007/s13197-014-1347-1.
[8] X.P. Huang, W.Q. Li, Y.M. Wang, F.X. Wan, Drying characteristics and quality of stevia rebaudiana leaves by far-infrared radiation, LWT – Food Sci. Technol. 140 (2021), https://doi.org/10.1016/j.lwt.2020.110638.
[9] Y.a. Zeng, Y. Liu, J. Zhang, H. Xi, X.u. Duan, Effects of far-infrared radiation temperature on drying characteristics, water status, microstructure and quality of kiwifruit slices, J. Food Meas. Charact. 13 (4) (2019) 3086–3096.
[10] L.J. Yuan, X. He, R. Lin, S.S. Cheng, Effect of ultrasonic pretreatment on moisture state and hot air drying characteristics of kiwifruit, J. Agric. Eng. 37 (13) (2021) 263–272.
[11] J. Szadzińska, C. Róa Biegańska-Marecik, et al., Ultrasound- and microwave-assisted convective drying of carrots – process kinetics and product's quality

analysis, Ultrasonics Sonochem. 48 (2018) 249–258, https://doi.org/10.1016/j.ultsonch.2018.05.040.
[12] H. Bozkir, A.R. Ergün, Effect of sonication and osmotic dehydration applications on the hot air drying kinetics and quality of persimmon, LWT- Food Sci. Technol. 131 (2020), https://doi.org/10.1016/j.lwt.2020.109704.
[13] B. Bwa, A. Xg, B. Hma, A. Cz, Enhancing jackfruit infrared drying by combining ultrasound treatments: effect on drying characteristics, quality properties and microstructure, Food Chem. 358 (2021).
[14] X. Shi, Y.u. Yang, Z. Li, X. Wang, Y. Liu, Moisture transfer and microstructure change of banana slices during contact ultrasound strengthened far-infrared radiation drying, Innov. Food Sci. Emerg. Technol. 66 (2020) 102537.
[15] H. Xi, Y. Liu, L. Guo, R. Hu, Effect of ultrasonic power on drying process and quality properties of far-infrared radiation drying on potato slices, Food Sci. Biotechnol. 29 (1) (2019), https://doi.org/10.1007/s10068-019-00645-1.
[16] M. Dubois, K.A. Gilles, J.K. Hamilton, P.A. Rebers, F. Smith, Colorimetric method for determination of sugars and related substances, Anal. Chem. 28 (3) (1956) 350–356, https://doi.org/10.1021/ac60111a017.
[17] V.M. Beato, F. Orgaz, F. Mansilla, A. Montaño, Changes in phenolic compounds in garlic (allium sativum l.) owing to the cultivar and location of growth, Plant Foods Human Nutrit. 66 (3) (2011) 218–223, https://doi.org/10.1007/s11130-011-0236-2.
[18] M. Lay, S. Karsani, S. Mohajer, S.A. Malek, Phytochemical constituents, nutritional values, phenolics, flavonols, flavonoids, antioxidant and cytotoxicity studies on phaleria macrocarpa (scheff.) boerl fruits, BMC Complem. Alternative Med. 14 (2014), https://doi.org/10.1186/1472-6882-14-152.
[19] C. Nencini, A. Menchiari, G.G. Franchi, L. Micheli, In vitro antioxidant activity of aged extracts of some italian allium species, Plant Foods Hum. Nutr. 66 (1) (2011) 11–16, https://doi.org/10.1007/s11130-010-0204-2.
[20] J. Chen, L. Tan, Y. Peng, J. Yang, Q. Zhang, L.H. Zhang, Study on optimization of whole bean curd coagulant formulation by response surface methodology, Chinese J. Cereals Oils 33 (05) (2018) 16–23.
[21] A. Nathakaranakule, P. Jaiboon, S. Soponronnarit, Far-infrared radiation assisted drying of longan fruit, J. Food Eng. 100 (4) (2010) 662–668.
[22] J.V. García-Pérez, C. OrtuiO, A. Puig, J.A. Carcel, I. Perez-Munuera, Enhancement of water transport and microstructural changes induced by high-intensity ultrasound application on orange peel drying, Food Bioprocess Technol. 5 (6) (2012) 2256–2265.
[23] Fratianni, Niro, Alam, MDR, Cinquanta, Di, et al. (2018). Effect of a physical pretreatment and drying on carotenoids of goji berries (lycium barbarian l.). *LWT-Food Sci Technol*, 2018, 92, 318-323. 10.1016/j.lwt.2018.02.048.
[24] Y. Gong, D.H. Liu, X. Wang, Correlation study of color and chemical composition of dried fruits of Lycium barbarum, Food Sci. Technol. 40 (10) (2015) 57–61.
[25] Q. Zhao, L.Y. Zhang, C.M. Qiu, Microwave vacuum drying characteristics study of Lycium barbarum polysaccharide extract and its quality analysis, Food Ind. Sci. Technol. 34 (23) (2013) 266–270.
[26] Y. Niwa, T. Kanoh, T. Kasama, M. Negishi, Activation of antioxidant activity in natural medicinal products by heating, brewing and lipophilization. a new drug delivery system, Drugs Exp. Clin. Res. 14 (5) (1988) 361, https://doi.org/10.2165/00003495-198800362-00009.
[27] S. Hamrouni, Rahali, F. Z. , Rebey, I. B. , Bourgou. (2013). Total phenolics, flavonoids, and antioxidant activity of sage (salvia officinalis l.) plants as affected by different drying methods. *Food Bioprocess Tech, 2013,6*(3), 806-817. 10.1007/s11947-012-0877-7.
[28] Y. Liu, C. Sun, Y. Lei, H. Yu, H. Xi, X.u. Duan, Contact ultrasound strengthened far-infrared radiation drying on pear slices: Effects on drying characteristics, microstructure, and quality attributes, Drying Technol. 37 (6) (2019) 745–758.
[29] A. Kaya, AydN, O., Kolayl, S. (2010). Effect of different drying conditions on the vitamin c (ascorbic acid) content of hayward kiwifruits (actinidia deliciosa planch). *Food & Bioproducts Process., 88*(2-3), 165-173. 10.1016/j.fbp.2008.12.00.
[30] F.X. Wan, W.Q. Li, Y. Luo, B. Wei, X.P. Huang, Effect of ultrasonic pretreatment on the characteristics and quality of far-infrared vacuum drying of Lycium barbarum, Chinese Herbal Med. 51 (18) (2020) 4654–4663.
[31] W. Yu, Jian, L. , Xuan, L. , Liu, Y. , Shao, L. , Ge, H. , et al. (2018). Astragalus root dry extract restores connexin43 expression by targeting mir-1 in viral myocarditis. *Phytomedicine, 46*, S0944711318302198, http://dx. doi.Org/10.1016/j.phymed.2018.06.031.
[32] M.L. Rojas, T.S. Leite, M. Cristianini, I.D. Alvim, P.E.D. Augusto, Peach juice processed by the ultrasound technology: changes in its microstructure improve its physical properties and stability, Food Res. Int. 82 (apr.) (2016) 22–33, https://doi.org/10.1016/j.foodres.2016.01.011.
[33] Y.H. Liu, X.F. Li, S. Miao, Y. Yin, W.K. Zhu, Ultrasonic-far-infrared radiation drying characteristics and microstructure of pumpkin slices, J. Agric. Eng. 32 (10) (2016) 10.
[34] Y. Pei, Z. Li, Xu, W., Song, C. , Song, F. (2021). Effects of ultrasound pretreatment followed by far-infrared drying on physicochemical properties, antioxidant activity and aroma compounds of saffron (crocus sativus l.). *Food Biosci., 42,* 101186. 10.1016/j.fbio.2021.101186.